

# Pressure-induced half-metallic gap transformation in $\text{Co}_2\text{MnSi}$ observed by tunneling conductance spectroscopy

M. Nobori, T. Nakano, J. Hasegawa, and G. Oomi

*Department of Physics, Kyushu University, Hakozaki 812-8581, Fukuoka, Japan*

Y. Sakuraba and K. Takanashi

*Institute for Materials Research, Tohoku University, Katahira 2-1-1, Aoba-ku, Sendai 980-8577, Japan*

Y. Miura

*Research Institute of Electrical Communication, Tohoku University, Katahira 2-1-1, Aoba-ku, Sendai 980-8577, Japan*

Y. Ohdaira and Y. Ando

*Department of Applied Physics, Graduate School of Engineering, Tohoku University, Aoba-yama 6-6-05, Aramaki, Aoba-ku, Sendai 980-8579, Japan*

(Received 7 October 2010; published 17 March 2011)

Applied hydrostatic pressure dependence of tunneling magnetoresistance (TMR) properties was investigated in magnetic tunnel junctions using the half-metallic Heusler alloy  $\text{Co}_2\text{MnSi}$  (CMS). The half-metallic electronic structure in CMS was observed by measuring tunneling-conductance spectroscopy under different applied pressure. The effect of tetragonal distortion in CMS on the electronic structure was also calculated on the basis of the first-principle density-functional method. The TMR ratio showed no remarkable variation with increasing pressure from ambient to 1.5 GPa. It was clearly found that the valence-band edge of the half-metallic gap moved toward the Fermi level with increasing pressure up to 1.8 GPa. These experimental results showed good qualitative agreement with the theoretical calculation of density of states of CMS at high pressure.

DOI: [10.1103/PhysRevB.83.104410](https://doi.org/10.1103/PhysRevB.83.104410)

PACS number(s): 75.76.+j

## I. INTRODUCTION

Application of high pressure is a unique method for obtaining important knowledge about the electronic properties of materials because the density of state (DOS), Fermi surface, bandwidth, as well as the volume and structure of the materials, etc., can be continuously controlled by applying high pressure. In the research field of spintronics, the effect of pressure on the giant magnetoresistance (GMR) of Fe/Cr, Co/Cu magnetic multilayers, and Co-Al-O insulating granular films has been investigated intensively, and some interesting results, such as an enhancement of GMR and tunnel magnetoresistance (TMR) have been observed.<sup>1-4</sup>

Half-metallic materials, which possess perfectly spin-polarized conduction electrons due to the energy band gap either in the spin-up or -down channel, have been extensively studied in recent spintronics, especially as ferromagnetic electrodes of magnetic tunnel junctions (MTJs)<sup>5-10</sup> and current-perpendicular-to-plane-GMR devices<sup>11-13</sup> in order to enhance magnetoresistance (MR) effects. A large TMR ratio of 560% was observed in the  $\text{Co}_2\text{MnSi}$  (CMS)-based MTJ with a conventional Al-O amorphous barrier at low temperature,<sup>5,6</sup> indicating a large spin polarization over 0.84 for the CMS electrode. The TMR ratio, however, drastically decreased to about 60% at room temperature (RT). Although the presence of non-quasi-particle states just above the half-metallic gap and a magnon excitation at the barrier interface are suggested as possible origins for a disappearance of half metallicity at RT,<sup>14,15</sup> the scale of the half-metallic gap and the position of the Fermi level ( $E_F$ ) in the half-metal gap are also important factors for determining MR characteristics at finite temperature and bias voltage in half-metal-based MTJs. Picozzi *et al.*

theoretically investigated the effect of hydrostatic pressure on the electronic structure in  $\text{Co}_2\text{MnX}$  ( $X = \text{Si}, \text{Ge}, \text{and Sn}$ ) and found an increase of the half-metallic band gap and progressive shifts of  $E_F$  from the valence band (VB) into the band gap by volume compression.<sup>16</sup> Hydrostatic pressure-induced non-half-metal to half-metal transition has also been predicted in PtMnSn by Galanakis *et al.*<sup>17</sup> Thus, it is very interesting to study how half-metallic electronic structures in Heusler alloys change by applying high pressure through a dependence of MR properties on pressure in the MTJs. The knowledge obtained from pressure dependence of MR properties can be interesting physically and also useful to clarify and to improve transport properties in the half-metal-based spintronics devices.

In this paper, we will report the hydrostatic pressure effects on the spin-dependent transport properties in the CMS-based MTJ. The pressure dependence of the spin polarization and the half-metallic gap structure in CMS was systematically investigated against pressure by measuring the TMR ratio and tunneling conductance spectroscopy. Furthermore, the present experimental results were compared with the theoretical calculations of the DOS under lattice distortion induced by a different hydrostatic pressure.

## II. SAMPLE PREPARATION

The sample was fabricated on a Cr-buffered MgO (001) single-crystalline substrate using a UHV-compatible magnetron sputtering system. A (001)-CMS layer grows epitaxially on a Cr(001)/MgO(001) substrate due to the small lattice mismatching. The stacking structure of the MTJ was MgO-substrate/Cr(40 nm)/CMS(30)//Al(1.3)-O/CoFe(5)/IrMn(10)/capping layers, which is same as that of

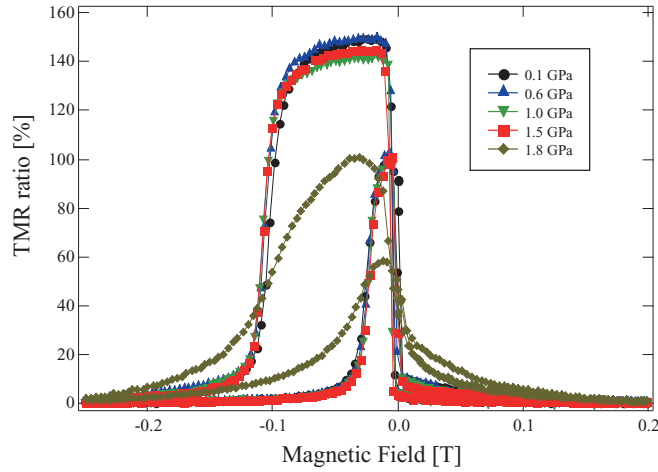


FIG. 1. (Color online) TMR ratio in CMS/Al-O/CoFe-MTJ as a function of magnetic field in hydrostatic pressure at 4.2 K.

the sample used in Ref. 6. The CMS layer was deposited at ambient temperature and was annealed at 500 °C to enhance the chemical ordering. From the structural evaluation using x-ray diffraction, (111) superlattice peak indicating  $L2_1$  ordering was clearly confirmed in the CMS. The IrMn antiferromagnetic layer induces a one-direction magnetic anisotropy for the CoFe upper electrode, which gives a clear antiparallel magnetization configuration between CMS and CoFe layers. The film was patterned into a pillar shape with  $50 \times 50 \mu\text{m}^2$  by photolithography and Ar-ion milling.

### III. EXPERIMENTAL METHOD

The magnetic field between  $-0.3 \text{ T} < B < 0.3 \text{ T}$  is applied to the direction of the parallel to the [110] in-plane direction of

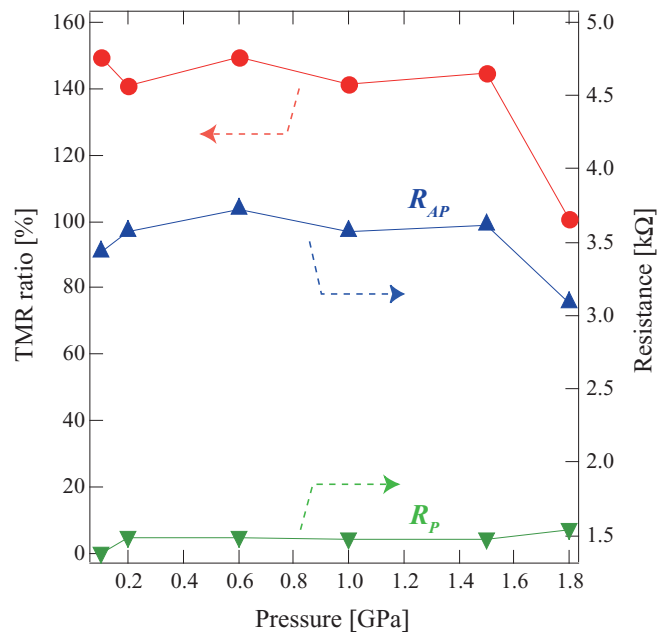


FIG. 2. (Color online) Pressure dependence of the TMR ratio and tunneling resistances in parallel and antiparallel states for CMS/Al-O/CoFe-MTJ at 4.2 K.

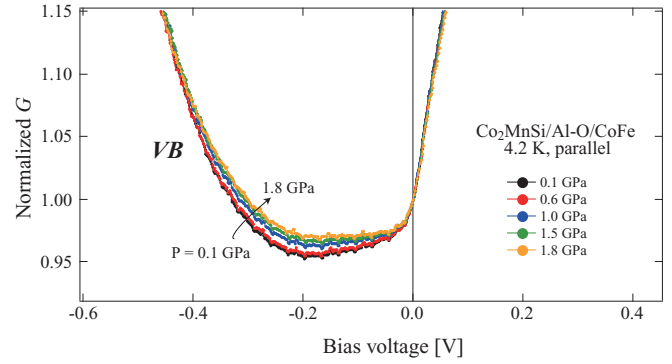


FIG. 3. (Color online) Bias voltage dependence of differential tunneling conductance  $G(dI/dV)$  of the parallel magnetic configuration in CMS/Al-O/CoFe-MTJ at 4.2 K.

the CMS layer, which corresponds to the easy magnetization direction of CMS. A MR effect was measured by a standard dc four-probe method at a bias voltage under 1 mV at 4.2 K. The applied bias voltage dependence of differential tunneling conductance  $G (= dI/dV)$  was measured using a nanovoltmeter (model 2182A; Keithley Instruments, Inc.) and a small current

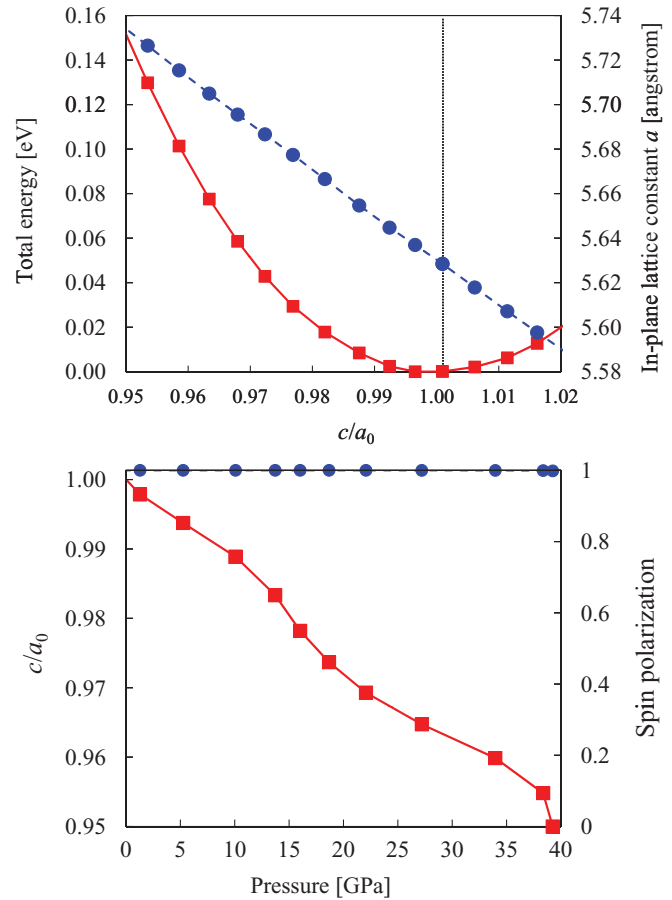


FIG. 4. (Color online) (a) The total energy [eV] (filled square points and solid line) and the optimized in-plane lattice constant  $a$  [Å] (filled circle points and broken line) of CMS as a function of the tetragonal distortion  $c/a_0$ . (b) The  $c/a_0$  and the spin polarization at the Fermi level in CMS as a function of the compressive pressure [GPa], where the in-plane lattice constant  $a$  is relaxed.

source (model 6221; Keithley Instruments, Inc.). When only the elastic tunneling process is considered in the CMS/Al-O/CoFe-MTJ,  $G$  is proportional to  $D_M^{\text{CMS}} D_M^{\text{CoFe}} + D_m^{\text{CMS}} D_m^{\text{CoFe}}$  in parallel configuration. Here,  $D_{M(m)}$  stands for the majority-(minority)-spin DOS at  $E_F$ . Thus, we can observe the half-metallic gap in CMS in a  $G$ - $V$  curve as well mentioned in Ref. 5. In this study, the positive bias voltage was applied to the bottom CMS electrode, i.e., the tunneling electron moves from the upper CoFe electrode to the CMS electrode at positive bias voltage. Hydrostatic pressure, which means uniaxial compressive pressure in the perpendicular direction for the stacking film plane, was generated using a hybrid CuBe-MP35N piston cylinder cell, which is equipped with a superconducting magnet.<sup>18</sup> The sample was placed inside the Teflon capsule, and Mg-O substrate were shaped to the inside diameter of the Teflon capsule to make it not lean when applying high pressure. The pressure inside the Teflon capsule was kept constant by automatically controlling the load of hydraulic press at 4.2 K. Daphne-oil 7373 was used as the pressure-transmitting medium.<sup>19</sup>

IV. RESULTS AND DISCUSSION

Figure 1 shows TMR curves of CMS/Al-O/CoFe-MTJ at 4.2 K in various pressures from  $P = 0.1$  to 1.8 GPa. The TMR ratio was defined as  $\delta R/R_P = (R_{\text{max}} - R_P)/R_P$ , where  $R_{\text{max}}$  and  $R_P$  are the tunneling resistance of the MTJ in the maximum and in the parallel magnetic configuration states, respectively. At ambient pressure ( $P = 0.1$  GPa), clear spin-valve behavior of the TMR with a plateau of an antiparallel state and a large TMR ratio of about 149% were obtained. The spin polarization of CMS, evaluated from Julliere’s model, was 0.85 by considering a reasonable assumption of  $P_{\text{CoFe}} = 0.50$  from previous studies.<sup>20,21</sup> The tunneling resistance in the

parallel magnetization states and the TMR ratio did not change remarkably with applied pressure up to 1.5 GPa. At 1.8 GPa, however, the shape of the TMR curve changed drastically, which lost a clear antiparallel plateau state and caused a large reduction in the TMR ratio of 100%. Since the pinning-field effect from IrMn and the rapid reversal of magnetization in CMS did not change from 1.5 to 1.8 GPa, a deterioration of the TMR curve was mainly ascribed to the deformation of the magnetization curve of CoFe by applying high pressure. Figure 2 shows pressure dependence of the TMR ratio and tunneling resistances in CMS/Al-O/CoFe-MTJ. As mentioned above, the reduction of the TMR ratio at 1.8 GPa is attributed not to the intrinsic reduction of spin polarization in CMS but to the incomplete antiparallel state of the TMR curve. Note that the tunneling resistance in the parallel state at 1.8 GPa did not change so much from that at 1.5 GPa, indicating no structural destruction in the Al-O tunneling barrier and no remarkable change in the electronic state, i.e., no destruction of half metallicity in CMS.

Figure 3 shows the normalized  $G$ - $V$  curves for CMS/Al-O/CoFe-MTJ in parallel magnetic configuration at various pressures. In Fig. 3, at the negative bias voltage region, the tunnel conductance ( $G$ ) increased suddenly around  $-0.3$  V (here defined as  $V_{\text{VB}}$ ) under every pressure, indicating that the VB edge in the half-metal gap of CMS is located about 0.3 V below  $E_F$ . In contrast to the negative bias region, the experimental  $G$ - $V$  curves on the positive bias voltage side were found to be independent of pressure despite large shifting of the conduction band (CB) edge with  $c/a$  distortion in the calculation shown in the inset of Fig. 5. In our recent study on the  $\text{Co}_2\text{MnAl}_x\text{Si}_{1-x}$ -based MTJs, the rapid increase in  $G$  at the small positive bias voltage region was also observed in every Al concentration  $x$  and thereby was explained by a dominant contribution of an

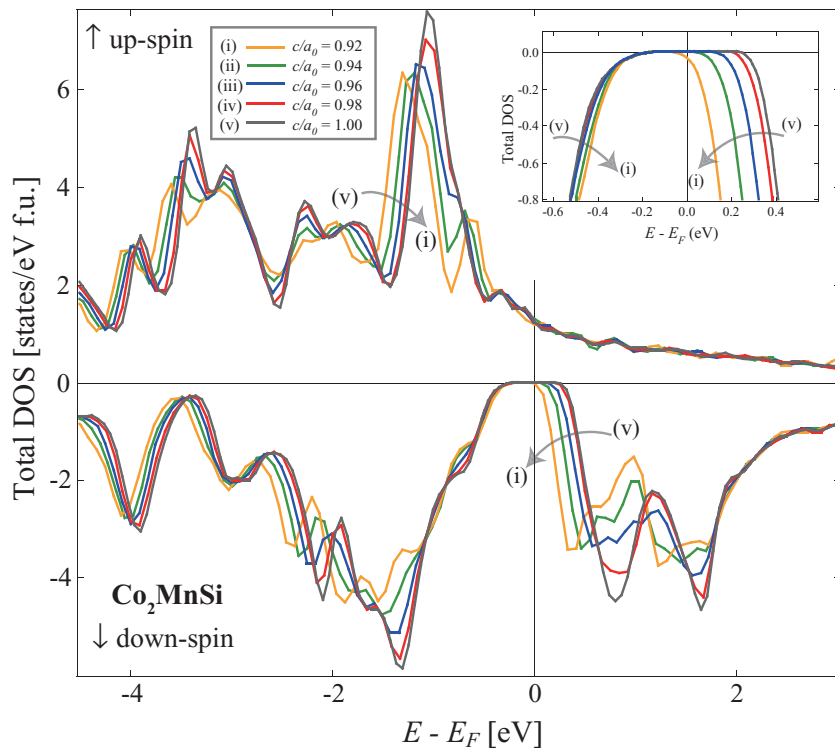


FIG. 5. (Color online) The total DOS of  $L1_0$ -CMS for the tetragonal distortion  $c/a_0 = 1.00-0.92$  ( $a_0 = 5.63$  [Å]), where the in-plane lattice constant  $a$  is relaxed. The inset shows the magnification of the total DOS of CMS near the Fermi level. The positive (negative) sign of the DOS indicates the majority-spin (minority-spin) states, respectively.

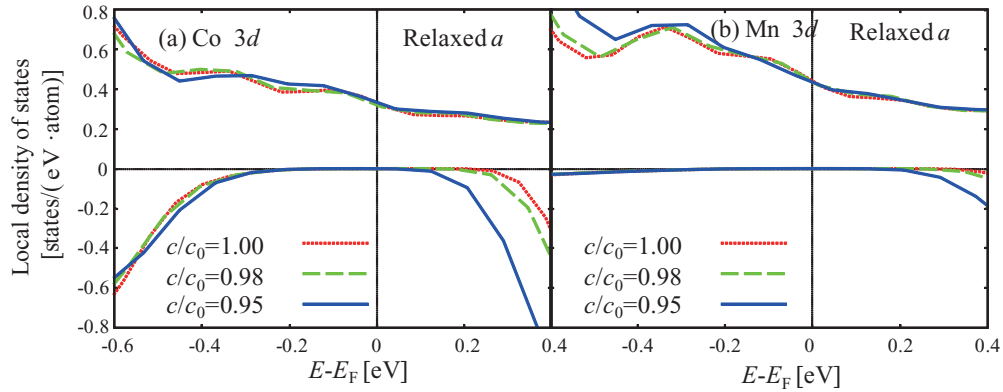


FIG. 6. (Color online) The LDOS projected onto the atomic orbital of (a) Co  $3d$  and (b) Mn  $3d$  in CMS for the tetragonal distortion  $c/a_0 = 1.00$  (dotted lines),  $0.98$  (dashed lines), and  $0.95$  (solid lines) where the in-plane lattice constant  $a$  is relaxed.

inelastic tunneling (IET) process at the positive bias voltage region.<sup>22</sup> Here, the IET process with a magnon excitation at the CMS interface was suggested as the most possible path of the IET for the positive bias voltage region because the exchange energy of Co in CMS at the tunneling barrier interface was predicted to be reduced so much compared with that inside CMS.<sup>23</sup> Thus, in the present observations in applied pressure dependence, a clear shift of an edge of a half-metallic gap with pressure seemed to be observed only at the negative bias region.

We investigated the pressure effect on the electronic structures of CMS theoretically on the basis of the first-principles density-functional calculation implemented in the Vienna

*ab initio* simulation package (VASP).<sup>24,25</sup> The exchange and correlation terms are treated within the spin-polarized generalized gradient approximation using the Perdew-Becke-Ernzerhof parametrization.<sup>26</sup> The nuclei and core electrons are described by the projector-augmented plane-wave potential,<sup>27,28</sup> and the wave functions are expanded in a plane-wave basis set with a cutoff energy of 337.3 [eV]. To evaluate the tetragonal distortion of CMS, the tetragonal unit cell with  $(a/\sqrt{2}) \times (a/\sqrt{2}) \times c$  is used in the calculations where  $a$  and  $c$  are in-plane and perpendicular lattice constants of CMS. The equilibrium lattice constant of the  $L2_1$ -type CMS, in the present calculation, is  $a = c = 5.63$  [Å] ( $\equiv a_0$ ). The Brillouin-zone integration is performed with a modified

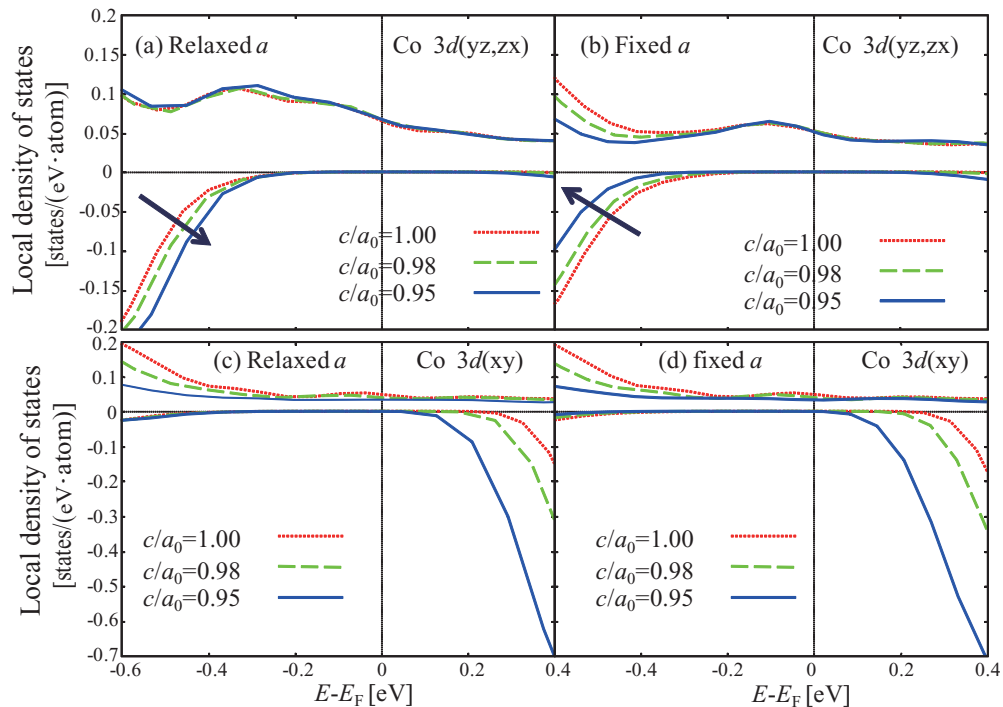


FIG. 7. (Color online) The LDOS projected onto the atomic orbital of Co  $3d_{yz}$  (or  $3d_{zx}$ ) in CMS for the tetragonal distortion  $c/a_0 = 1.00$  (dotted lines),  $0.98$  (dashed lines), and  $0.95$  (solid lines) ( $a_0 = 5.63$  [Å]), with (a) the relaxed in-plane lattice constant  $a$  and (b) the fixed in-plane lattice constant  $a$ . The LDOS projected onto the atomic orbital of Co  $3d_{xy}$  in CMS for the tetragonal distortion  $c/a_0 = 1.00$  (dotted lines),  $0.98$  (dashed lines), and  $0.95$  (solid lines), with (c) relaxed  $a$  and (d) fixed  $a$ .

tetrahedron method with Blöchl corrections<sup>29</sup> on the uniform  $15 \times 15 \times 11$  mesh.

First, we calculated the total energy and the optimized in-plane lattice constant  $a$  of CMS as a function of the tetragonal distortion  $c/a_0$ . As can be seen in Fig. 4(a), the in-plane lattice constant  $a$  (filled circle points) increases with decreasing  $c/a_0$  owing to the relaxation of atomic positions along the in-plane direction against the compressive distortion of CMS. Then, we evaluated the compressive-pressure dependence of  $c/a_0$  and the spin polarization at the Fermi level in CMS. In Fig. 4(b), it is found that the change of  $c/a_0$  against the uniaxial compressive pressure perpendicular to the (001) face of CMS (filled square points) is about  $-0.05$  by 40 [GPa], resulting from a relatively large bulk modulus of CMS.<sup>30</sup> The spin polarization at the Fermi level takes almost unity for the pressure up to 40 [GPa], indicating that electronic structures of CMS near the Fermi level do not change against the compressive pressure. This result is qualitatively consistent with the present observation shown in Figs. 1 and 2, i.e., no variation of spin polarization against pressure from 0.1 to 1.5 Pa.

Figure 5 shows the total DOS of  $L1_0$ -CMS for  $c/a_0 = 1.00 - 0.92$  ( $a_0 = 5.63$  [Å]). The magnification of the total DOS near the Fermi level is shown in the inset of Fig. 5. The half-metallic character of  $\text{Co}_2\text{MnSi}$  is preserved within this compressive distortion region, however, the minority-spin energy gap near the Fermi level becomes narrower with decreasing  $c/a_0$ , where both VB and conduction band edges move toward the Fermi level in the minority-spin state. Observed monotonic shifts of  $V_{\text{VB}}$  toward small bias voltage with increasing applied pressure in Fig. 3 shows good qualitative agreement with this calculation. To look at the electronic structures in more detail, in Figs. 6(a) and 6(b), we present the local density of states (LDOS) projected onto the atomic orbital of Co  $3d$  and Mn  $3d$ . It is found that the change of the LDOS near the Fermi level owing to the compressive pressure is significant for Co  $3d$  rather than for Mn  $3d$ . Since the half-metallic gap in the minority-spin state of CMS near the Fermi level is mainly constructed by the bonding and antibonding features of the second nearest-neighbor Co-Co  $3d$  interaction, the pressure effect near the Fermi level is clearly observed for the LDOS of Co  $3d$  as compared with the LDOS of Mn  $3d$ .

From detailed analysis on the LDOS of Co  $3d$ , we found that the change in the minority-spin VBs near the Fermi level by the compressive pressure occurs more clearly in the LDOS of Co  $3d_{yz}$  (or  $3d_{zx}$ ), while the change in the conduction bands appears mainly in the LDOS of Co  $3d_{xy}$ . Figures 7(a) and 7(c) show the LDOS of Co  $3d_{yz}$  (or  $3d_{zx}$ ) and Co  $3d_{xy}$  in  $\text{Co}_2\text{MnSi}$  for  $c/a_0 = 1.00, 0.98, \text{ and } 0.95$ . The LDOS of Co  $3d_{yz}$  (or  $3d_{zx}$ ) and Co  $3d_{xy}$  for the fixed in-plane lattice constant  $a$  are also shown in Figs. 7(b) and 7(d) as a reference. In Fig. 7(a), it is found that the minority-spin VB edge moves toward the Fermi level, while in Fig. 7(b) (in the case of fixed  $a$ ), it moves away from the Fermi level with decreasing  $c/a_0$ . On

the other hand, as shown in Figs. 7(b) and 7(d), the conduction band edge in the LDOS of Co  $3d_{xy}$  moves toward the Fermi level with decreasing  $c/a_0$  in both relaxed and fixed  $a$ . These results indicate that the effect of the compressive pressure to the minority-spin DOS of CMS near the Fermi level can be attributed to the relaxation of atomic position along the in-plane direction. The relaxation owing to the compressive pressure increases the in-plane bond length between Co atoms and weakens the second nearest-neighbor Co-Co  $3d_{yz}$  (or  $3d_{zx}$ ) hybridization. This reduces the bonding and antibonding features of the second nearest-neighbor Co-Co  $3d$  interaction, making the half-metallic gap narrower with decreasing  $c/a_0$ .

According to Figs. 3–5, however, the experimentally observed shift of  $V_{\text{VB}}$  is relatively large since an application of pressure below 1.8 GPa corresponds to the small change in  $c/a$  from 1.00 to 0.99 in the calculation. Thus, it is speculated that larger shifts of  $V_{\text{VB}}$ , with pressure other than that expected, may originate from a considerable tetragonal transformation in the CMS layer by a strong distortion effect multiplied from the neighboring Cr buffer layer, Al-O barrier, and/or MgO substrate in the stacking MTJ structure. Additionally, in order to obtain a more quantitative agreement between the experiment and the calculation, we need to consider a distortion effect at the CMS/Al-O interface because the TMR effect is sensitive to the ferromagnetic layer/tunneling barrier interface.

## V. SUMMARY

In this paper, the hydrostatic pressure effects for the spin-dependent transport properties have been investigated in the half-metallic CMS-based MTJ. The applied pressure dependence of the spin polarization and the half-metallic gap structure in CMS was systematically investigated against pressure by measuring a TMR ratio with tunneling conductance spectroscopy. A large TMR ratio did not change by applying pressure from 0.1 to 1.5 GPa because the half-metallic gap of CMS is preserved within this pressure range. However, we detected a slight shift in the VB edge of the half-metallic gap toward  $E_F$ , which showed good qualitative agreement with our prediction on the basis of first principles. Our calculation found that the relaxation of atomic position along the in-plane direction by the compressive pressure was the origin of the observed shifting of the VB edge in the half-metallic minority-gap in CMS.

## ACKNOWLEDGMENTS

The authors thank S. Mitani for providing the opportunity to start this collaborating work. This work was supported by Grants-in-Aid for Scientific Research in Priority Area “Creation and control of spin current” (Grant No. 19048004) and Young Scientists (B) (Grant No. 20760005) from MEXT, Japan.

<sup>1</sup>G. Oomi, Y. Uwatoko, Y. Obi, K. Takanashi, and H. Fujimori, *J. Magn. Magn. Mater.* **126**, 513 (1993).

<sup>2</sup>G. Oomi, T. Sakai, Y. Uwatoko, K. Takanashi, and H. Fujimori, *Physica B* **239**, 19 (1997).

- <sup>3</sup>S. Kaji, G. Oomi, S. Mitani, S. Takahashi, K. Takanashi, and S. Maekawa, *Phys. Rev. B* **68**, 054429 (2003).
- <sup>4</sup>K. Suenaga, S. Higashihara, M. Ohashi, G. Oomi, M. Hedo, Y. Uwatoko, K. Saito, S. Mitani, and K. Takanashi, *Phys. Rev. Lett.* **98**, 207202 (2007).
- <sup>5</sup>Y. Sakuraba, M. Hattori, M. Oogane, Y. Ando, H. Kato, A. Sakuma, and T. Miyazaki, *Appl. Phys. Lett.* **88**, 192508 (2006).
- <sup>6</sup>Y. Sakuraba, J. Nakata, M. Oogane, Y. Ando, H. Kato, A. Sakuma, and T. Miyazaki, *Jpn. J. Appl. Phys.* **44**, L1100 (2005).
- <sup>7</sup>S. Tsunegi, Y. Sakuraba, M. Oogane, K. Takanashi, and Y. Ando, *Appl. Phys. Lett.* **93**, 112506 (2008).
- <sup>8</sup>D. Ebke, J. Schmalhorst, N.-N. Liu, A. Thomas, G. Reiss, and A. Hütten, *Appl. Phys. Lett.* **89**, 192506 (2006).
- <sup>9</sup>T. Ishikawa, T. Marukame, H. Kijima, K.-I. Matsuda, T. Uemura, M. Arita, and M. Yamamoto, *Appl. Phys. Lett.* **89**, 192505 (2006).
- <sup>10</sup>N. Tezuka, N. Ikeda, F. Mitsunashi, and S. Sugimoto, *Appl. Phys. Lett.* **94**, 162504 (2009).
- <sup>11</sup>T. Furubayashi, K. Kodama, H. Sukegawa, Y. K. Takahashi, K. Inomata, and K. Hono, *Appl. Phys. Lett.* **93**, 122507 (2008).
- <sup>12</sup>Y. Sakuraba, K. Izumi, T. Iwase, S. Bosu, K. Saito, K. Takanashi, Y. Miura, K. Futatsukawa, K. Abe, and M. Shirai, *Phys. Rev. B* **82**, 094444 (2010).
- <sup>13</sup>T. Iwase, Y. Sakuraba, S. Bosu, K. Saito, S. Mitani, and K. Takanashi, *Appl. Phys. Express* **2**, 063003 (2009).
- <sup>14</sup>L. Chioncel, Y. Sakuraba, E. Arrigoni, M. I. Katsnelson, M. Oogane, Y. Ando, T. Miyazaki, E. Burzo, and A. I. Lichtenstein, *Phys. Rev. Lett.* **100**, 086402 (2008).
- <sup>15</sup>M. Yamamoto, T. Ishikawa, T. Taira, G.-f. Li, K.-i. Matsuda, and T. Uemura, *J. Phys.: Condens. Matter* **22**, 164212 (2010).
- <sup>16</sup>S. Picozzi, A. Continenza, and A. J. Freeman, *Phys. Rev. B* **66**, 094421 (2002).
- <sup>17</sup>I. Galanakis, S. Ostanin, M. Alouani, H. Dreysse, and J. M. Wills, *Phys. Rev. B* **61**, 4093 (2000).
- <sup>18</sup>F. Honda, S. Kaji, I. Minamikawa, M. Ohashi, G. Oomi, T. Eto, and T. Kagayama, *J. Phys. Condens. Matter* **14**, 11501 (2002).
- <sup>19</sup>K. Yokogawa, K. Murata, H. Yoshino, and S. Aoyama, *Jpn. J. Appl. Phys.* **46**, 3636 (2007).
- <sup>20</sup>M. Julliere, *Phys. Lett.* **54A**, 225 (1975).
- <sup>21</sup>F. Han, M. Oogane, H. Kubota, Y. Ando, and T. Miyazaki, *Appl. Phys. Lett.* **77**, 283 (2000).
- <sup>22</sup>Y. Sakuraba, K. Takanashi, T. Kota, T. Kubota, M. Oogane, A. Sakuma, and Y. Ando, *Phys. Rev. B* **81**, 144422 (2010).
- <sup>23</sup>A. Sakuma, Y. Toga, and H. Tsuchiura, *J. Appl. Phys.* **105**, 07C910 (2009).
- <sup>24</sup>G. Kresse and J. Hafner, *Phys. Rev. B* **47**, 558 (1993).
- <sup>25</sup>G. Kresse and J. Furthmüller, *Comput. Mater. Sci.* **6**, 15 (1996); *Phys. Rev. B* **54**, 11169 (1996).
- <sup>26</sup>P. Perdew, K. Burke, and M. Ernzerhof, *Phys. Rev. Lett.* **77**, 3865 (1996).
- <sup>27</sup>E. Blöchl, *Phys. Rev. B* **50**, 17953 (1994).
- <sup>28</sup>G. Kresse and D. Joubert, *Phys. Rev. B* **59**, 1758 (1999).
- <sup>29</sup>E. Blöchl, O. Jepsen, and O. K. Andersen, *Phys. Rev. B* **49**, 16223 (1994).
- <sup>30</sup>S. Picozzi, A. Continenza, and A. J. Freeman, *Phys. Rev. B* **66**, 094421 (2002).